

Beam propagation of x rays in a laser-produced plasma and a modified relation of interferometry in measuring the electron density

Hong Guo,* Timon Chengyi Liu, Xiquan Fu, Wei Hu, and Song Yu

Laboratory of Light Transmission Optics, South China Normal University, Guangzhou 510631, People's Republic of China

(Received 26 December 2000; published 15 May 2001)

In this paper, using a quantum mechanical technique and introducing the so-called V representation (where the representation transformation is made by using the potential Hamiltonian V), we studied x-ray propagation in a linear plasma medium both analytically and numerically. A modified relation between the phase of the probe and the reference light and the electron density of the plasma is derived, in which the contribution of the gradient of the electron density has been taken into account. It is shown that this relation has the advantage in measurements of the electron density of a plasma using the x-ray interferometry technique of lessening the errors originating from the electron density gradient. The validity of x-ray interferometry is discussed in both mathematical and physical terms.

DOI: 10.1103/PhysRevE.63.066401

PACS number(s): 52.70.La, 41.20.Jb

I. INTRODUCTION

Measurement of the laser-plasma electron density plays an important role in the diagnostics of laser-produced plasmas, and the method of the refractive index of the plasma medium [1–7] is one of the methods used extensively. Early work used visible and uv light as the probe and more recently x-ray sources came to be popular because of their special characteristics, such as (i) high critical density so that higher electron density measurements become possible; (ii) a refractive index close to unity and a small diffraction effect; (iii) a short wavelength which increases the resolution; and (iv) reduction of the high absorption near the critical surface [3–9]. Further, narrow-bandwidth multilayer optics can be used so that the detector can avoid being swamped by the spontaneous emission of the plasma [6,7]. The x-ray probe propagates in the collisionless plasma under measurement, the refractive index of which is

$$N = \left(1 - \frac{n_e}{n_c} \right)^{1/2}, \quad (1)$$

where n_e is the electron density of the plasma, $n_c = 1.1 \times 10^{21} \lambda^{-2} \text{ cm}^{-3}$ (with λ in μm) is the critical electron density per cubic centimeter, λ is the wavelength of the x-ray probe, and the reference light propagates in free space ($N = 1$). The difference in optical length between the probe and the reference light is $\Delta L = \int_0^L (N - 1) dz$ [1,3,8]. Application of the interferometric technique in measuring the electron density is based upon the fact that, after passing through the plasma, the probe light has a phase difference $\Delta\Phi = \omega\Delta L/c$ relative to the reference light [supposing the probe and reference light are plane waves, then after passing through the plasma, the reference light field is $E_r(z) = E(0)\exp(ikz)$, while the probe light field is $E_p(z) = E(0)\exp(ikz + i\Delta\Phi)$, and $\Delta\Phi$ is connected to the electron density n_e via the relation [1]

$$\Delta\Phi = - \frac{\omega}{2cn_c} \int_0^L n_e dl, \quad (2)$$

where the integral is taken along the propagation route L of the probe beam. Equation (2) is the basis of x-ray interferometry for measuring the electron density of a plasma and we will refer to it as the conventional relation in the following discussion. Thus n_e can be inferred from a measurement of the phase difference $\Delta\Phi$ obtained by interference of the probe and reference light. Equation (2) can be derived theoretically from the optical path difference or by the Wentzel-Kramers-Brillouin-Jeffreys (WKBJ) (and hence essentially geometrical optical) approximation, in which the electron density gradient is ignored. This is valid for most cases of underdense plasma measurement.

Although the above relation has been used extensively, one finds that there are some differences between the experimental and theoretical results. In this paper, we intend to modify the relation given by Eq. (2) by taking into account the gradient of the electron density. From Maxwell's equations, together with Eq. (1), it can be seen that $\vec{\nabla} \cdot \vec{E}$ is proportional to $\vec{\nabla} n_e$ [10] and can generally be ignored; hence we can safely assume that the x-ray probe propagating in a plasma medium is linearly polarized monochromatic light and can be depicted by a paraxial scalar field, i.e., $E(x, y, z) = \psi(x, y, z) \exp[i(kz - \omega t)]$. Then the equation for x-ray beam propagation in a linear plasma medium reads

$$2ik \frac{\partial \psi}{\partial z} + \nabla_{\perp}^2 \psi - \frac{n_e}{n_c} k^2 \psi = 0, \quad (3)$$

where k is the wave number of the x-ray probe in vacuum ($k = \omega/c = 2\pi/\lambda$). Equation (3) is a Schrödinger equation with inhomogeneous potential, which has no analytical solution, and therefore the relation between n_e and $\Delta\Phi$ cannot be derived explicitly. However, we will show that by applying some well-developed techniques of quantum mechanics, such as the bra and ket depiction, the representation transformation, etc., a more accurate relation between n_e and $\Delta\Phi$ can be derived.

*Electronic address: hguo@scnu.edu.cn

The paper is organized as follows. In Sec. II, we use quantum mechanical techniques to reinvestigate Eq. (3) and introduce the so-called V representation (where the representation transformation is made by using the potential Hamiltonian V) to derive a modified relation between n_e and $\Delta\Phi$. In Sec. III numerical simulations are carried out, and we compare our results obtained using the modified analytical results and using the conventional results of Eq. (2) to those obtained from a full numerical calculation based on Eq. (3). In Sec. IV a discussion and conclusion are given.

II. DERIVATION OF THE MODIFIED RELATION

In the following discussion, the field ψ is viewed as a ket state $|\psi(z)\rangle$ evolving with the propagation distance z ; then Eq. (3) can be rewritten as

$$ib \frac{\partial}{\partial z} |\psi(z)\rangle = H |\psi(z)\rangle, \quad (4)$$

where

$$b = k^{-1} = \frac{\lambda}{2\pi}, \quad H = H_0 + V, \quad H_0 = -\frac{b^2}{2} \nabla_{\perp}^2, \quad V = \frac{n_e}{2n_c}.$$

Introducing the unitary operator $U_V = \exp(-ib^{-1} \int_0^z V dz)$ and transforming the state $|\psi(z)\rangle$ and physical variable F in the Schrödinger representation to another representation (denoted as the V representation hereafter), i.e.,

$$|\psi_V(z)\rangle = U_V^{-1} |\psi(z)\rangle, \quad F_V = U_V^{-1} F U_V, \quad (5)$$

gives

$$ib \frac{\partial}{\partial z} |\psi_V(z)\rangle = H_{0V} |\psi_V(z)\rangle, \quad (6)$$

where $H_{0V} = U_V^{-1} H_0 U_V$. Equation (6) depicts the ‘‘free space’’ propagation of the probe in the V representation. (See Fig. 1, showing the reference and probe light propagating in free space in the Schrödinger representation and the V representation, respectively.) One then derives

$$|\psi_V(z)\rangle = T \exp\left(-ib^{-1} \int_0^z H_{0V} dz\right) |\psi_V(0)\rangle, \quad (7)$$

where T is the time-ordering operator [11] and $T(H_{0N})^m = H_{0V}(z_1) H_{0V}(z_2) \cdots H_{0V}(z_m)$, ($z_1 < z_2 < \cdots < z_m$). If $\forall l \neq m$, one has

$$[H_{0V}(z_l), H_{0V}(z_m)] = 0; \quad (8)$$

then $T=1$ and can be removed from Eq. (7). Since, in the discussions within this paper, $V/H_0 \sim 10^{-4} \ll 1$ and so Eq. (8) is always valid, we will neglect this operator. It can be justified that $U_V(0) = 1$, and hence $|\psi_V(0)\rangle = |\psi(0)\rangle$; therefore

$$|\psi(z)\rangle = U_V T \exp\left(-ib^{-1} \int_0^z H_{0V} dz\right) |\psi(0)\rangle. \quad (9)$$

By using the Baker-Hausdorff lemma [11], i.e.,

$$\begin{aligned} & \exp(iG\eta) A \exp(-iG\eta) \\ &= A + i\eta [G, A] + \frac{i^2 \eta^2}{2!} [G, [G, A]] + \cdots \\ &+ \frac{i^n \eta^n}{n!} [G, [G, \cdots [G, A] \cdots]] + \cdots, \end{aligned} \quad (10)$$

where A and G are operators and η is a real parameter, and setting $A = H_0$, $G = \int_0^z V dz$, $\eta = b^{-1}$, one has

$$\begin{aligned} H_{0V} &= H_0 + \frac{1}{2} \left(\int_0^z dz \vec{\nabla}_{\perp} V \right)^2 + ib \int_0^z dz \vec{\nabla}_{\perp} V \cdot \vec{\nabla}_{\perp} \\ &+ i \frac{b}{2} \int_0^z dz \nabla_{\perp}^2 V. \end{aligned} \quad (11)$$

It should be noted that Eq. (11) includes the contributions of all terms mentioned in Eq. (10) (which is an infinite series) whereas all the higher order terms of η^n ($n \geq 3$) are equal to zero due to the commutation relations $[\nabla_{\perp}^2 V, V] = 0$.

Next, we evaluate the magnitude of the terms of H_{0V} to give the solution of $|\psi(z)\rangle$. Suppose the propagation length of the x-ray probe is L (thickness of the plasma medium) and the probe has the beam width W , then according to the Lagrange theorem one has

$$\begin{aligned} \frac{H_{0V}}{V} &\sim \frac{H_0}{V} + \frac{VL^2}{2W^2} [\vec{\nabla}_{\perp} \ln V(\xi_1, \vec{r})]^2 + i \frac{bL}{W^2} \vec{\nabla}_{\perp} \\ &\times \ln V(\xi_2, \vec{r}) \cdot \vec{\nabla}_{\perp} + i \frac{bL}{2W^2} \\ &\times \{ \vec{\nabla}_{\perp}^2 \ln V(\xi_3, \vec{r}) + [\vec{\nabla}_{\perp} \ln V(\xi_3, \vec{r})]^2 \}, \end{aligned} \quad (12)$$

where $\xi_i \in [0, L]$, $i = 1, 2, 3$, and $\vec{\nabla}_{\perp}$ is the dimensionless transverse gradient operator. If all of the electron density gradient terms are ignored, then Eq. (12) gives

$$H_{0V} \approx H_0. \quad (13)$$

By connecting Eqs. (9) and (13) one derives

$$|\psi(z)\rangle \approx U_V U_0 |\psi(0)\rangle, \quad (14)$$

where $U_0 = \exp(-ib^{-1} \int_0^z H_0 dz)$. Since $|\psi(z)\rangle = U_0 |\psi(0)\rangle$ is the field of reference light, then from Eq. (14) one finds that the difference between the reference and probe lights lies in the phase factor

$$U_V(L) = \exp\left(-ib^{-1} \int_0^L V dl\right).$$

The phase corresponding to the interference can be derived as

$$\Delta\Phi = -\frac{\omega}{2cn_c} \int_0^L n_e dl,$$

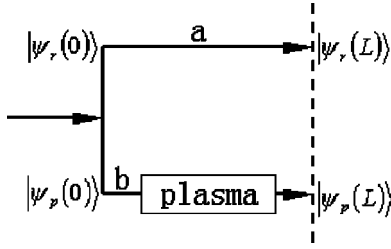


FIG. 1. Schematic setup of the x-ray interferometric technique to measure the laser-plasma electron density, in which route *a* is the reference light evolving from $|\psi_r(0)\rangle = |\psi(0)\rangle$ to $|\psi_r(L)\rangle = U_0|\psi(0)\rangle$ while *b* is the x-ray probe evolving from $|\psi_p(0)\rangle = |\psi(0)\rangle$ to $|\psi_p(L)\rangle = U_V T \exp(-ib^{-1} \int_0^L H_0 V dz) |\psi(0)\rangle$. ‘‘a’’ and ‘‘b’’ show the propagation of reference and probe light in free space in Schrödinger and *V* representation, respectively.

which is just Eq. (2) the result obtained under the WKBJ approximation [1].

Next we consider the lowest order electron density gradient term, which is described by the second term on the right-hand side of Eq. (11), with the order of $O(L/W^2)$, while the third and fourth terms are of $O(L/(kW^2)) \ll O(L/W^2)$. From this point of view, after passing through plasma over the distance *L*, the probe field $|\psi_p(L)\rangle$ becomes

$$|\psi_p(L)\rangle \approx \exp\left[-ib^{-1} \int_0^L \left[V + \frac{1}{2} \left(\int_0^L \vec{\nabla}_\perp V dt'\right)^2\right] dl\right] \times U_0 |\psi(0)\rangle, \quad (15)$$

while the reference light $|\psi_r(L)\rangle$ becomes

$$|\psi_r(L)\rangle = U_0 |\psi(0)\rangle \quad (16)$$

(see Fig. 1). Therefore the modified phase difference can be derived as

$$\begin{aligned} \Delta\Phi &= -b^{-1} \int_0^L \left[V + \frac{1}{2} \left(\int_0^L \vec{\nabla}_\perp V dt'\right)^2\right] dl \\ &= -\frac{\omega}{2cn_c} \left[\int_0^L n_e dl + \frac{1}{4n_c} \int_0^L \left(\int_0^L \vec{\nabla}_\perp n_e dt'\right)^2 dl \right]. \end{aligned} \quad (17)$$

Equation (17) is the modified relation between the electron density and the phase difference. In the following section, we will carry out some numerical simulations, based on Eq. (2), Eq. (17), and the direct simulation using Eq. (3), and make a comparison among them.

III. NUMERICAL SIMULATIONS

For the sake of clarity we will denote the phases evaluated by Eqs. (2), (17), and (3) as $\Delta\Phi_A$, $\Delta\Phi_B$, and $\Delta\Phi_0$, respectively. Here Eq. (2) is referred to as the conventional relation (CR), Eq. (17) as the modified relation (MR), and Eq. (3) as the experimental relation (ER). The errors of the CR and MR relative to the ER are defined as

$$\delta_{A,B} = \left| \frac{\Delta\Phi_{A,B} - \Delta\Phi_0}{(\Delta\Phi_0)_{\max}} \right|. \quad (18)$$

Before the numerical simulations, we first give some brief analysis for a special case. Suppose the wavelength of the x-ray probe is $\lambda = 15.5$ nm and the electron density distribution is cylindrically symmetric (the symmetry axis is the *y* axis) and has a Gaussian profile, i.e.,

$$n_e(r) = \frac{n_c}{A} \exp\left(-\frac{\pi r^2}{w_0^2}\right),$$

where $r = \sqrt{x^2 + z^2}$ and n_c/A and w_0 denote the peak value and the normalization parameter of the electron density distribution, respectively. Then Eqs. (2) and (17) yield

$$\Delta\Phi_A = -\frac{\pi w_0}{A\lambda} \exp\left(-\frac{\pi x^2}{w_0^2}\right) \operatorname{erf}\left(\frac{L\sqrt{\pi}}{2w_0}\right) \quad (19)$$

and

$$\begin{aligned} \Delta\Phi_B &= -\left[\frac{\pi w_0}{A\lambda} \exp\left(-\frac{\pi x^2}{w_0^2}\right) \operatorname{erf}\left(\frac{L\sqrt{\pi}}{2w_0}\right) + \frac{\pi^3 V_c x^2}{A^2 \lambda w_0^4} \right. \\ &\quad \left. \times \exp\left(-2\frac{\pi x^2}{w_0^2}\right) \right], \end{aligned} \quad (20)$$

where $\operatorname{erf}(x) = 2\pi^{-1/2} \int_0^x \exp(-t^2) dt$ is the error function, and

$$\begin{aligned} V_c &= \frac{w_0^2}{2\pi} \left\{ \operatorname{erf}\left(\frac{L\sqrt{\pi}}{2w_0}\right) \left[2w_0 \exp\left(-\frac{L^2\pi}{4w_0^2}\right) + \pi L \operatorname{erf}\left(\frac{L\sqrt{\pi}}{2w_0}\right) \right] \right. \\ &\quad \left. - \sqrt{2} w_0 \operatorname{erf}\left(\frac{L}{w_0} \sqrt{\frac{\pi}{2}}\right) \right\} \end{aligned}$$

is the characteristic volume. For $L/w_0 > 3$ one has $V_c \approx Lw_0^2/2 - 0.225w_0^3$. In the following simulations, we choose $\lambda = 15.5$ nm and $w_0 = 1.0$ mm. Equation (3) is solved by a split Fourier transform algorithm [12] and Eqs. (2) and (17) by iteration. The errors of the CR and MR are shown in Fig. 2, Fig. 3, and Fig. 4, while the electric field distribution of the x-ray probe after passing through the plasma is shown in Fig. 5.

Figure 2 shows a comparison of the errors in the conventional and modified relations, where $A = 100.0$ and $L/w_0 = 10$. From this one finds that (i) there are five zeros ($x/w_0 = 0, \pm 0.4$, and $\pm\infty$) for curve *b* but two ($x/w_0 = 0$ and $\pm\infty$) for curve *a*; and (ii) $x_1/w_0 = 0$ is the point where $\vec{\nabla}_\perp n_e(x_1) = \vec{0}$, which is the same as the case of $n_e = \text{const}$; (iii) $x_2/w_0 = \pm 0.4$ is the point where $\vec{\nabla}_\perp n_e(x_2) = [\vec{\nabla}_\perp n_e(x)]_{\max}$, and $\delta_A(x_2) = [\delta_A(x_2)]_{\max}$, while $\delta_B(x_2)$ turns out to be zero; (iv) $x_3/w_0 = \pm\infty$ is the point where the plasma is very dilute. Figure 3 is similar to Fig. 2 except that n_e is assumed to take a third-order super-Gaussian profile,

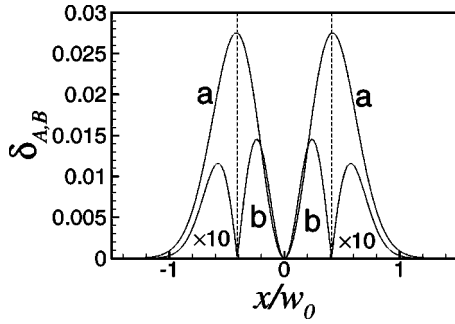


FIG. 2. Comparison of the errors due to the conventional and modified formulas when n_e is a Gaussian profile and $A=100.0$, $L/w_0=10$. Curves a and b denote the dependence of δ_A and δ_B ($\times 10$) on the normalized transverse coordinate x/w_0 , respectively. It can be seen that (i) there is no error for either δ_A or δ_B at the origin; (ii) when δ_A takes its maximum value (which is also the point for $\vec{\nabla}_\perp n_e$ to take its maximum value), i.e., $x/w_0 \approx 0.4$, $\delta_B = 0$.

i.e., $n_e(x,z) = n_c \exp\{-[\pi(x^2+z^2)/w_0^2]^3\}/A$, $L/w_0=5$, and the maximum point of the electron density gradient is $x/w_0 \approx \pm 0.5$, where δ_B vanishes.

Figure 4 shows a comparison of the maximum errors in the conventional and modified relations when n_e is Gaussian profile and $A=100.0$, with different propagation lengths L/w_0 . Curves a and b denote the dependence of δ_A and δ_B ($\times 5$) on the normalized longitudinal coordinate L/w_0 , respectively. The figure indicates that (i) $(\delta_B)_{\max} \ll (\delta_A)_{\max}$; and (ii) $(\delta_B)_{\max}$ varies more rapidly than $(\delta_A)_{\max}$ with L/w_0 .

Figure 5 shows the intensity distribution of the x-ray probe after passing through the plasma. The electron density has a Gaussian profile, $L/w_0=5$, and curves a , b , c , and d denote the cases of $A=100.0, 200.0, 1000.0$, and 10000.0 , respectively. It is evident that (i) the tendency of the variation of the curves is similar and they have an intersection point (x_1) that gives the maximum value of the divergence of the field, i.e., $\vec{\nabla} \cdot \vec{E}(x_1) = [\vec{\nabla} \cdot \vec{E}(x)]_{\max}$; (ii) for the dilute plasma case, i.e., when A is large, the field varies slowly and

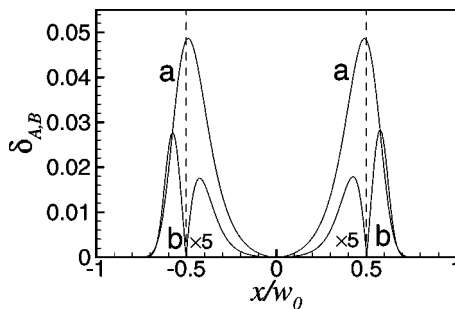


FIG. 3. Comparison of the errors due to the conventional and modified formulas when n_e is a third-order super-Gaussian profile, i.e., $n_e(x,z) = n_c \exp\{-[\pi(x^2+z^2)/w_0^2]^3\}/A$, where $A=100.0$ and $L/w_0=5$. Curve a and b denote the dependence of δ_A and δ_B ($\times 5$) on the normalized transverse coordinate x/w_0 , respectively. It can be seen that (i) there is no error for either δ_A or δ_B at the origin; (ii) when δ_A takes its maximum value (which is also the point for $\vec{\nabla}_\perp n_e$ to take its maximum value), i.e., $x/w_0 \approx 0.5$, $\delta_B = 0$.

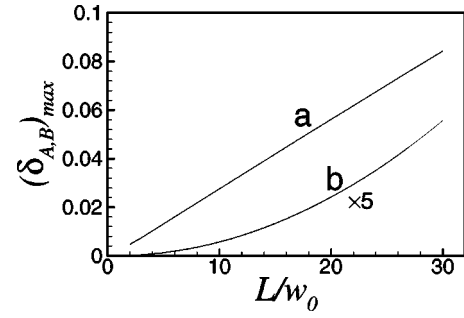


FIG. 4. Comparison of the maximum errors due to the conventional and modified formulas when n_e is a Gaussian profile and $A=100.0$, with different L/w_0 . Curves a and b denote the dependence of δ_A and δ_B ($\times 5$) on the normalized longitudinal coordinate L/w_0 , respectively. The figure indicates that (i) $(\delta_B)_{\max} \ll (\delta_A)_{\max}$; and (ii) $(\delta_B)_{\max}$ varies more rapidly than $(\delta_A)_{\max}$ with L/w_0 .

hence the contribution due to the divergence of the field can be ignored.

From the above simulations, one finds the following. (i) The errors in the conventional relation are mainly owing to the contribution of the electron density gradient, i.e., $\vec{\nabla}_\perp n_e$, and will take the maximum value when the electron density gradient is maximum. (ii) The MR proposed in this paper can overcome the errors due to the electron density gradient and, in particular, the errors from the MR vanish when the electron density gradient takes its maximum value. (iii) For the zero point of the gradient of the electron density and the very dilute plasma case, both methods are accurate. The CR is good enough and can in fact simplify the evaluation. (iv) Normally for the underdense plasma it can be shown that $\vec{\nabla} \cdot \vec{E} \propto \vec{\nabla}_\perp n_e$; therefore the electron density gradient plays an important role so far as the validity of Eq. (3) and hence of the x-ray interferometry is concerned.

IV. DISCUSSION AND CONCLUSION

From the analytical investigations mentioned above, one can derive the conditions for validity of x-ray interferometry.

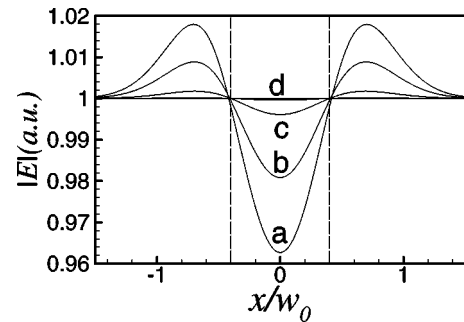


FIG. 5. Intensity distribution of the x-ray probe after passing through the plasma. The electron density has a Gaussian profile, $L/w_0=5$, curves a , b , c , and d denote the cases of $A=100.0, 200.0, 1000.0$, and 10000.0 , respectively. It is evident that (i) the tendency of the variation of the curves is similar and they have two points of intersection which give the biggest gradient of the field; (ii) for a dilute plasma, i.e., A is large, the field varies slowly and hence the contribution due to the gradient of the field can be ignored.

First, the electron density gradient should be, on the one hand, sufficiently small so that $\vec{\nabla} \cdot \vec{E}$ can be ignored, and, on the other hand sufficiently large so that the contribution to the errors of the CR is significant, which is the very basic requirement of interferometry. Secondly, a further relation can be derived for the validity of the interferometric technique for the CR which, in the following discussions, appears to be the connection between the CR and MR. From the equations governing the probe light ψ_p propagation in plasma and the reference light ψ_r propagation in free space (see Fig. 1), i.e.,

$$2ik \frac{\partial \psi_r}{\partial z} + \nabla_{\perp}^2 \psi_r = 0,$$

$$2ik \frac{\partial \psi_p}{\partial z} + \nabla_{\perp}^2 \psi_p - \frac{n_e}{n_c} k^2 \psi_p = 0, \quad (21)$$

where ψ_r and ψ_p are connected by $\psi_p = \psi_r \exp(i\Delta\Phi_0)$ ($\Delta\Phi_0$ is the phase corresponding to the interference of the two lights and has been used to compare the errors in this paper), one comes to

$$2 \frac{\partial \Delta\Phi_0}{\partial z} + \frac{n_e k}{n_c} = 0, \quad (22)$$

or equivalently

$$\Delta\Phi_0(z) = -b^{-1} \int_0^z V dz. \quad (23)$$

It can be found from Eqs. (22) and (23) (the conditions for the validity of interferometry meteorologically) that (i) mathematically, the phase operator $\exp[i\Delta\Phi_0] = U_V$ can be used as a unitary operator for the representation transformation; (ii) after the transformation the propagation of the x-ray probe in the plasma can be treated as a ‘‘free space’’ propagation and only the free Hamiltonian in the representation H_{0V} needs to be considered to evaluate the evolution of light.

Numerical simulations show that the MR presented in this paper gives rise to a great reduction of the errors originating from the electron density gradient compared with the CR. In particular, when the electron density gradient takes its maximum value the error of the MR vanishes while that of the CR is a maximum. Hence this method can be used to measure the laser-plasma electron density in a more precise way. A schematic procedure for an algorithm using the Able transformation [1], i.e.,

$$n_e(r) = \mathcal{A}\{\Delta\Phi\} = -\frac{2cn_c}{\pi\omega} \int_r^{L/2} \frac{d\Delta\Phi}{dx} \frac{dx}{(x^2 - r^2)^{1/2}}, \quad (24)$$

where \mathcal{A} denotes the Abel transformation, together with the MR realized by the iteration algorithm, to derive the electron density in a more precise way is shown in Fig. 6, in which MT means the modified term $\delta\Phi$ and AT means Abel’s transformation. The basic idea of the procedure is as follows. (i) Derive a coarse value of the electron density from the measured phase $\Delta\Phi_0$ based on the AT, i.e., $n_e^0 = \mathcal{A}\{\Delta\Phi_0\}$;

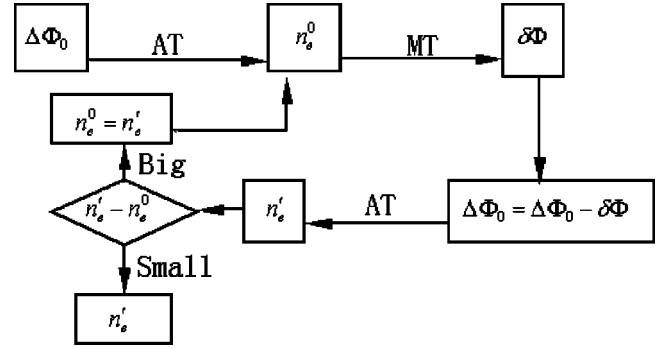


FIG. 6. Procedure for deriving a more precise value of the electron density based on Abel’s transformation, together with the modified relation derived in this paper, in which MT means the modified term $\delta\Phi$ and AT means Abel’s transformation.

then (ii) put n_e^0 into the MR to derive a modified value of the phase $\Delta\Phi_{\text{mod}} = \Delta\Phi_0 + \delta\Phi(n_e^0)$, where

$$\delta\Phi(n_e^0) = -\frac{\omega}{8cn_c^2} \int_0^L \left(\int_0^l \vec{\nabla}_{\perp} n_e^0 dl' \right)^2 dl.$$

Finally (iii) use the AT on the new phase $\Delta\Phi_{\text{mod}}$ to derive a new electron density, i.e., $n_e' = \mathcal{A}\{\Delta\Phi_{\text{mod}}\}$; then a more precise value of the electron density can be derived. It should be pointed out that the iteration should be done continuously until stability of the electron density is attained.

It should also be noted that, besides the merit of reducing the errors by taking into account the modified terms that we have derived and analyzed within the paper, the method we presented also implies that the measurement can be done for any paraxial beam for both reference and probe light, while the conventional method requires that the light should be plane wave.

In summary, by using a quantum mechanical technique and introducing the V representation, we have studied x-ray propagation in a linear plasma medium both analytically and numerically. A modified relation between the phase corresponding to the interference of the probe and reference light and the laser-plasma electron density is derived. Comparison of the modified relation with the conventional one is made and shows its merit of reducing the errors by considering the contribution of the gradient of the electron density.

ACKNOWLEDGMENTS

This work was partially supported by the Key Project of the National Natural Science Foundation of China (Grant No. 69789801), the Hong Kong RGC Earmarked Research Grant No. HKUST 6176/99P, the Key Project of the Natural Science Foundation of Guangdong Province (Grant No. 970842), the Team Project of Guangdong Provincial Department of Science and Technology (Grant No. 2003061), the funds of the National Hi-Tech Committee, the Fok Ying Tung Education Foundation (Grant No. 71058), and the Foundation for Key Young Teachers of the Ministry of Education of China. Dr. H. Pu is also acknowledged for his careful reading and some suggestions on the revised manuscript.

- [1] I.H. Hutchinson, *Principles of Plasma Diagnostics with Microwaves* (Cambridge University Press, Cambridge, England, 1987).
- [2] H. Soltwisch, in *Nuclear Fusion and Plasma Physics*, edited by Y.P. Huo, C.S. Liu, and F. Wagner (World Scientific, Singapore, 1995).
- [3] L.B. Da Silva *et al.*, Phys. Rev. Lett. **74**, 3991 (1995).
- [4] R. Cauble *et al.*, Phys. Rev. Lett. **74**, 3816 (1995).
- [5] C.H. Moreno *et al.*, Phys. Rev. E **60**, 911 (1999).
- [6] A.S. Wan *et al.*, J. Opt. Soc. Am. B **13**, 447 (1996).
- [7] A.S. Wan *et al.*, Phys. Rev. E **55**, 6293 (1997).
- [8] D. Ress *et al.*, Science **265**, 514 (1994).
- [9] R.A. London, Phys. Fluids **31**, 184 (1988).
- [10] See, e.g., W.L. Kruer, *The Physics of Laser-Plasma Interactions* (Addison-Wesley, Reading, MA, 1988).
- [11] See, e.g., J.J. Sakurai, *et al.*, *Advanced Quantum Mechanics* (Benjamin/Cummings, New York, 1985).
- [12] Govind P. Agrawal, *Nonlinear Fiber Optics*, 2nd ed. (Academic Press, San Diego, 1995).